Experiment and Numerical Simulation study of Trilateral Load of Ultra-high Performance Concrete Pipe

Lei He[1], Li Zhou[2] , Shanqing Ma[*1] , Wei Wang[2] , Yuan Lu[1] , Zengli Shi[1]

[1] China Electric Power Research Institute, Beijing 102401, China
[2.] State Grid Hubei Electric Power Co., Ltd. Economic and Technical Research Institute, Wuhan 430000, China

*Corresponding author: Shanqing Ma
E-mail address: dfeor5139rfj92@163.com

Abstract. This research examined the mechanical characteristics and failure patterns of ultra-high performance concrete (UHPC) pipe through trilateral loading test and numerical simulation. The test results provided critical data, including crack load, failure load, and load-displacement curves. The findings indicate that the crack load for the tested pipe is 232kN/m, the failure load is 452kN/m, the maximum horizontal displacement is 64.3mm, and the maximum vertical displacement is 71.6mm. During radial loading, four primary cracks and multiple secondary cracks emerged internally and externally on the left and right sides of the pipe top and bottom, ultimately leading to concrete spalling, reinforcing steel yielding, and compression zone concrete crushing. Using the test results, a finite element model for the trilateral test of the UHPC pipe was created using ABAQUS numerical software. When compared to the test results, the simulation results showed that the numerical method accurately predicted the macroscopic failure process and load-bearing capacity of the UHPC pipe.

Keywords: Pipe; UHPC; Trilateral load test; Mode of failure; Numerical simulation

1 Introduction

With urbanization and infrastructure development accelerating, the safety and durability of underground pipe have emerged as critical urban development issues. Traditional concrete pipe, often compromised by material deficiencies, complex construction environments, and other factors, experience cracking, leakage, and even failure, disrupting pipe operations and urban safety. Consequently, research now focuses on developing new pipe materials with enhanced strength, durability, and crack resistance[1-3].

Inorganic Ultra High Performance Fiber Reinforced Concrete (UHPC), a novel high-performance concrete, exhibits promising potential in structural engineering due to its superior mechanical properties, durability, and construction performance. Through optimized particle grading, ultrafine active admixtures, efficient admixtures, and microfine steel fiber toughening, UHPC surpasses ordinary concrete in compressive strength,

G. Zhao et al. (eds.), *Proceedings of the 2024 6th International Conference on Civil Architecture and Urban Engineering (ICCAUE 2024)*, Advances in Engineering Research 262,
https://doi.org/10.2991/978-94-6463-688-8_51

tensile strength, and toughness. These attributes broaden its application scope in bridges, tunnels, pipelines, and other engineering fields[4-6].

In pipe engineering, UHPC pipe are anticipated to address traditional concrete pipe issues and enhance pipeline bearing capacity and service life. However, studies on UHPC pipe mechanical properties are limited, particularly experimental research on full-scale models. Therefore, conducting trilateral load tests and in-depth analysis of UHPC pipe mechanical properties and failure modes is crucial for advancing UHPC applications in pipeline engineering.

Yan Xinyu et al.[7] studied C50 concrete and UHPC pipe joints, finding that larger eccentricity reduced bending stiffness but the gap narrowed with increased axial force. UHPC joints had higher bending stiffness and shear strength than C50 joints.

Liu Libin[8] investigated UHPC pipe, discovering steel-reinforced pipe had higher load-carrying capacity and deflection than unreinforced ones. Their ultimate load was 1.32 times the cracking load.

Yang Yan et al.[9] designed a UHPC pipe corridor, reducing maintenance time, joint count, construction period, and whole-life costs significantly.

Lu Li[10] measured deformation of UHPC-reinforced cross-sections using DIC, finding UHPC controlled deformation and increased load-carrying capacity by 30.1%.

Chen Renpeng et al.[11] analyzed UHPC-reinforced shield tube sheets, finding adhesive damage and that increasing reinforcement improved cracking resistance.

Liu Xian et al.[12] tested reinforced shield tunnel lining structures, revealing UHPC's tensile and compressive properties were less affected by humidity, increased initial stiffness, and improved the elastic limit.

Zhang Yang et al.[13] conducted flexural tests on damaged RC beams with UHPC reinforcement, finding prestressed UHPC layers improved stress state, inhibited cracks, and increased cracking load and flexural capacity.

Mi Zhou et al.[14] proposed a new pile foundation combining UHPC with PHC pipe piles, evaluating CIP and PA connection methods. CIP-connected piles had strong horizontal bearing capacity, while PA-connected piles had good self-resetting ability and high ductility.

Liao JinJing et al.[15] investigated UHPC pipe reinforced with FRP grids, finding FRP grids increased initial cracking load by 30%. Increasing pipe thickness and applying a CFRP jacket improved ring stiffness.

Adil M. Jabbar et al.[16] analyzed ordinary concrete beams reinforced with UHPC layers using Abaqus, focusing on layer arrangement, bonding methods, thickness, and reinforcement ratio. Increasing UHPC layer area, thickness, or reinforcement ratio enhanced bearing capacity.

In order to study the mechanical properties of ultra-high performance concrete composite pipe, the trilateral load test method was used to analyze the crack development, failure process and load-displacement curve of the pipe during the radial loading process. The mechanical properties and failure mechanism of UHPC pipe were revealed, and the calculation model of pipe bearing capacity was established to verify the results of the trilateral load test.

2 Trilateral Load Test

2.1 Test Pipe

The specifications of the test pipe are detailed below: an inner diameter of 2.5 meters, a wall thickness measuring 180 millimeters, featuring double reinforcement with an outer configuration of 10 @120 and an inner configuration of 10 @100. The outer protective layer has a thickness of 30 millimeters, while the inner protective layer is 25 millimeters thick. The pipe is constructed from C150 ultra-high performance fiber composite concrete. The steel bars used are of HRB400 grade, possessing a tensile strength standard value of 400 MPa and an elastic modulus of 200 GPa. The arrangement of the steel bars within the pipe is illustrated in Figure 1.

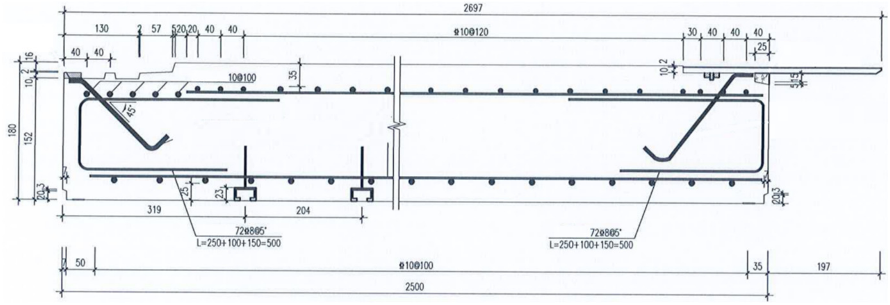

Fig. 1. Layout drawing of pipe steel bar(unit: mm).

2.2 2.2 Test method

Trilateral load test of the pipe section is carried out by referring to GB/T 16752-2017' Concrete and Reinforced Concrete Drainage Pipe Test Method'. The test device is composed of a test machine frame, a loading device and an instrument displaying the value, as shown in Figure 2. and Figure 3. In the figure : P is the radial loading load value ; f is the total load value ; L is the effective length of the pipe (the socket pipe is the length of the full-length Lp or cylindrical unit of the straight section) ; Dw is the outer diameter of the pipe.

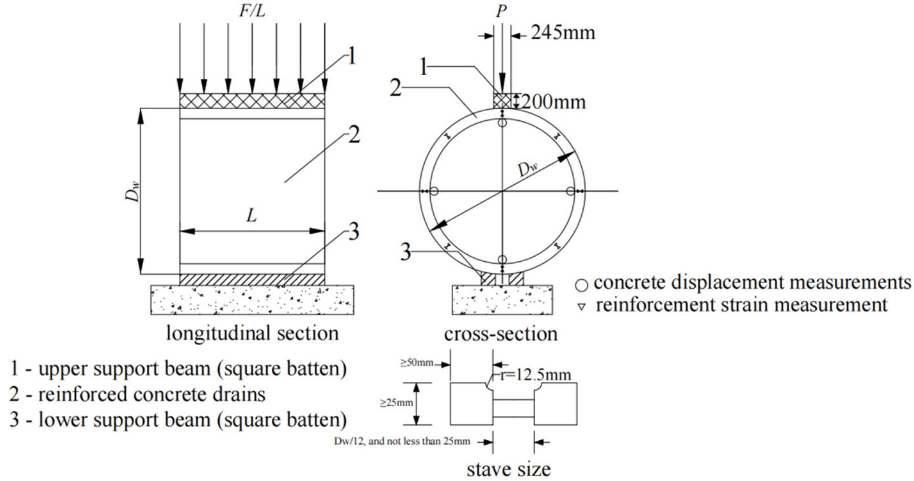

Fig. 2. Trilateral load test schematic diagram.

Fig. 3. Trilateral load test device.

2.3 Test results

(1) Pipe deformation and load

The load-displacement image of the pipe is shown in Figure 4. In the figure, Δx represents the horizontal displacement during the loading process of the pipe monitoring section, and Δy represents the vertical displacement during the loading process of the pipe monitoring section.

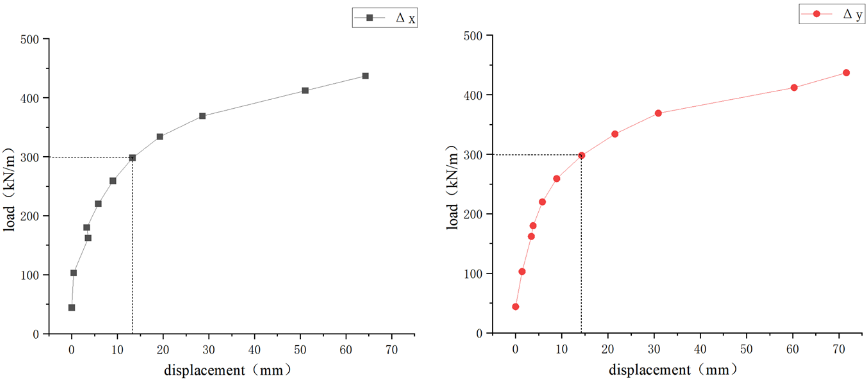

(a) Horizontal load-displacement curve (b) Vertical load-displacement curve

Fig. 4. Load-displacement curves in horizontal and vertical directions of pipe.

It can be seen from Figure 4. that the displacement deformation of the pipe in both the horizontal (Δx) and vertical (Δy) directions can be broadly categorized into two phases:

① Initially, during the early stages of loading, specifically when the load is below 300kN/m, the displacement in both horizontal and vertical directions of the pipe increases essentially in tandem with the load, maintaining a linear deformation relationship.

②When the load exceeds 300kN/m, the horizontal and vertical displacements of the pipe section increase faster than the previous elastic deformation stage. This is because when the load reaches 220kN/m, the pipe section cracks. With the increase of load, the cracks in all directions of the pipe section continue to develop to the structural stability failure of the pipe section, so that the deformation of the pipe section increases rapidly.

When the load reaches 412 kN/m, the displacement in the horizontal and vertical directions of the pipe increases rapidly compared with the previous load, and the pipe structure is close to failure. As the load increases, the displacement increment is larger than before. When the failure occurs, the maximum displacement in the horizontal direction of the pipe reaches 64.3 mm, and the vertical displacement reaches 71.6 mm.

The distribution and depth development of cracks are shown in Figure 5. The 0°, 90°, 180°and 270°in the diagram represent the top, right, bottom and left of the segment, respectively. When loaded to 220 kN/m, cracks first appear on the top of the pipe, and then cracks appear at the bottom of the pipe and on the left and right sides, but their distribution range is small. As the load intensifies, cracks emerging at the top and bottom of the pipe section diverge from the arch line. Once the load surpasses 334 kN/m, no further cracks form at the top of the pipe section, whereas cracks continue to emerge at the bottom until the pipe section reaches its failure load. As the load increases, the area covered by cracks on the left and right sides of the pipe section continually expands. When the pipe section attains its utmost bearing capacity, the crack distribution on the left and right sides spans nearly 90°.

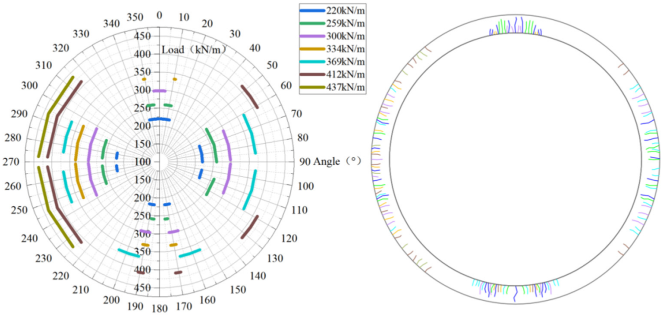

(a) Distribution of cracks produced by various levels of loading (b) Overall crack distribution

Fig. 5. Distribution of cracks in pipe joints under different loads.

(a) Pipe top (b) Right side of the pipe

Fig. 6. Cracking and damage of pipe.

As shown in Figure 6. In general, under radial loading conditions, cracks at the top and bottom of the pipe tend to concentrate more significantly, primarily appearing in the early to middle stages of loading. Conversely, cracks on the left and right sides of the pipe exhibit a broader distribution range and are more prominent during the middle to late stages of loading. As the load increases, the cracks at the top and bottom of the pipe primarily widen, whereas those on the left and right sides not only increase in number but also spread over a larger area. Notably, the cracks on the pipe's lateral sides are numerous, relatively short in length, and widely distributed. This phenomenon may be attributed to the steel fibers within the pipe material, which effectively distribute the stress over a larger area, thereby reducing the localized tensile stress in the concrete.

Furthermore, the steel fibers exhibit a notable capacity to mitigate the propagation of crack widths.

3 Numerical Simulation Analysis of Pipe

3.1 Numerical Simulation Model

The numerical finite element model depicting the trilateral load test of the pipe with ABAQUS is presented in Figure 7. This model fundamentally comprises two primary components: a concrete pipe and a steel cage. The dimensions and reinforcement ratio of the pipe align with those utilized in prior experimental setups. After conducting trials and assessments involving various element types and mesh densities, it has been established that the optimal simulation for the concrete pipe involves the use of eight-node hexahedral solid incompatible elements (C3D8I elements), offering enhanced precision while minimizing computational expenses. The steel cage, on the other hand, is modeled using two-node three-dimensional truss elements (T3D2 elements). Furthermore, to simulate the interaction between the steel reinforcement and the concrete pipe, an embedded region contact is employed. During the test, the reinforced concrete pipe section adopts a simply supported configuration, necessitating the application of a translational restraint at the base of the lower support beam. Additionally, a reference point is coupled to the top surface of the upper loading beam to facilitate the control of displacement loading and the monitoring of the resultant concentrated force acting on the pipe section.

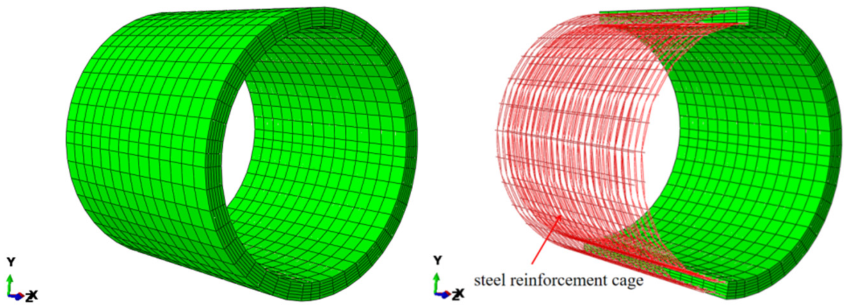

(a) Pipe (b) Pipe and steel reinforcement cage

Fig. 7. Finite element numerical model.

3.2 Material Parameters

The UHPC Concrete was employed Damage Plasticity(CDP) model in ABAQUS software and parameters were the same as Song Bin et al. applied[17].

In addition to the intrinsic parameters also need to choose the plasticity parameters of concrete. Referring to the research of existing scholars, the values of specific parameters are shown in Table 1.

Table 1. Other plasticity parameters.

α/°	E_c/MPa	Poisson's ratio for concrete	eccentricity	f_{b0}/f_{c0}	k_c	μ
38°	45300	0.2	0.1	1.16	0.667	0.0001

Table: α - expansion angle

E_c - modulus of elasticity of concrete;

f_{b0}/f_{c0} - ratio of compressive to tensile strength of concrete in both directions.

k_c - ratio of second stress invariant of tensile meridian and compressive meridian at initial yielding

μ - viscous parameter

The steel collar were modeled using an elastic model, with a modulus of elasticity of 200000 MPa, a density of 7850 kg/m^3, and a Poisson's ratio of 0.3.

3.3 Numerical Simulation Result

Load Displacement Curve.

The load-displacement curves of test pipe is shown in Figure 8. Observing the load-displacement curve, it is evident that following the peak load in the numerical simulation, the curve declines gradually. This is attributed to the simulation capturing the fiber effect through the macroscopic behavior of fiber-reinforced concrete, but neglecting the spatially non-uniform distribution of fibers and the fiber pull-out failure as cracks propagate, leading to discrepancies in the curve shape. Prior to reaching the peak load, the displacement-load curve of the numerical simulation aligns closely with the trilateral load test results. The peak load from the numerical simulation is 418.74 kN/m, with a 4.2% error compared to the ultimate load obtained from trilateral load test. The finite element method offers a reasonable representation of the load-bearing and deformation characteristics of ultra-high-performance concrete pipe.

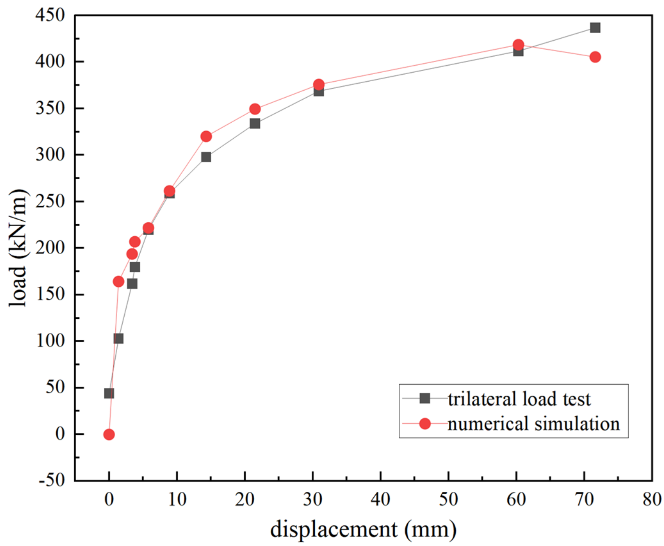

Fig. 8. Load-displacement curves of trilateral load test and numerical simulation.

The Failure Mode of Pipe.

Using the numerical simulation results from this set of experimental tubes as a reference, analyze that the critical sections of the tube during the loading process through stress distribution maps. When the vertical displacement at the top of the pipe reaches 71 mm in the simulation, Figure 9 depicts the stress map of the pipe joint, where S11 represents the horizontal stress (X-direction) and S22 represents the vertical stress (Y-direction). From this figure, it is evident that during the loading process, the concrete at the top and bottom of the pipe section experiences compression on the outer wall and tension on the inner wall. At this point, the concrete at the top of the pipe section reaches its peak tensile strength of 6.4 MPa, while the concrete on both sides experiences tension on the outer wall and compression on the inner wall, with a maximum tensile stress of 2.49 MPa, which remains within the elastic range. This suggests that the top concrete reaches the plastic damage stage of tension earlier than the concrete on both sides. When the vertical displacement at the top of the pipe reaches approximately 8.5 mm, the concrete on the outer walls of both sides of the pipe section attains its peak tensile strength and transitions into the plastic stage. At this stage, the maximum Mises stress of the concrete in the pipe section is 8.94 MPa (Figure 10), which is significantly lower than the compressive strength of the concrete, indicating that tensile cracks will first form in the tensile zone of the pipe section during the three-point bending test.

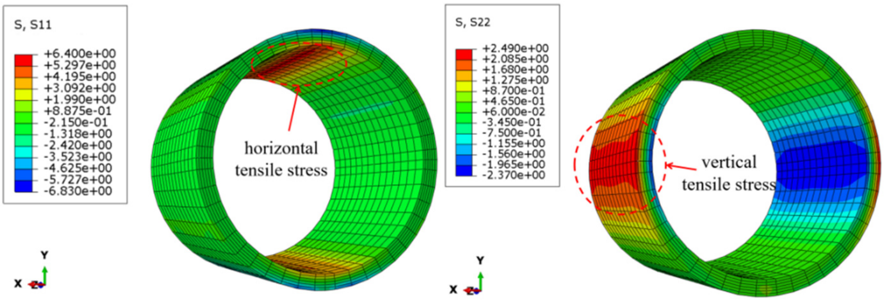

(a) Horizontal stress (b) Vertical stress

Fig. 9. The stress cloud diagram when the concrete of the pipe top reaches the tensile strength.

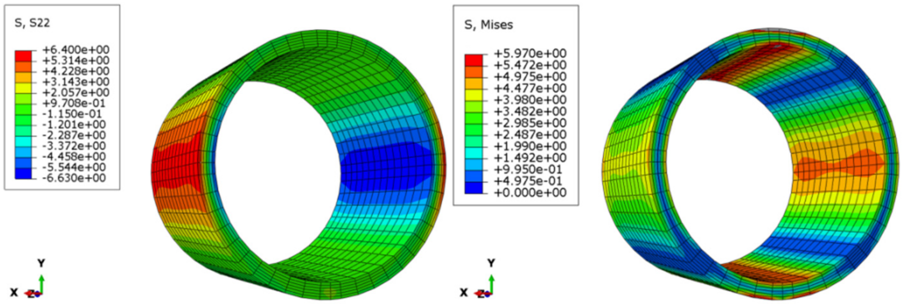

(a) Horizontal stress (b) Mises stress

Fig. 10. The stress cloud diagram when the waist concrete reaches the tensile strength.

4 Conclusion

In this study, the mechanical properties of ultra-high performance concrete (UHPC) pipe were systematically studied through trilateral load test and numerical simulation analysis, and the following main results were obtained :

(1) The deformation and failure laws of UHPC pipe under radial and axial loading are revealed. The trilateral load test of the bearing capacity of UHPC pipe was completed. By accurately controlling the loading conditions and monitoring methods, the failure mode, deformation and internal steel strain of the pipe section under radial loading conditions were obtained. The maximum displacement in the horizontal direction of the pipe joint reaches 64.3mm, and the maximum displacement in the vertical direction reaches 71.6mm. Four main cracks and multi-stage secondary cracks appear, and finally the concrete peels off, the steel bar yields, and the concrete in the compression zone crushes.

(2) ABAQUS is used to calculate the load-displacement curve of the finite element model of the pipe section under the condition of radial loading, and the cracking failure mode of the pipe section is obtained, and the model is verified. It is concluded that the

macroscopic failure process and bearing capacity of UHPC pipe can be reasonably predicted by finite element numerical simulation.

To sum up, this study has carried out a comprehensive and in-depth research on the mechanical properties of UHPC pipe by combining the bearing performance test and numerical simulation analysis. The research results have enriched the application technology system of UHPC in pipeline engineering and provided scientific basis and technical support for the design, construction and application of UHPC pipe. However, the mechanical properties of UHPC pipe under different geological conditions have not been explored. Future research can further explore the mechanical properties of UHPC pipe under different geological conditions, burial depths and loads, and develop more efficient and environmentally friendly preparation processes and construction methods, so as to promote the wide application and development of UHPC in the field of pipeline engineering.

Acknowledgments

This research is supported by the technology program of State Grid Co., Ltd. of China (No.5200-202322138A-1-1-ZN)

References

1. Cheng, X. L., Mu, R., & Liu, X. Y. Research progress on the preparation and mechanical properties of ultra-high performance concrete. Bulletin of the Chinese Ceramic Society,1-21.
2. Chen, M., Feng, J., & Zhang, T. Study on dynamic splitting tensile properties of ultra-high performance concrete after high temperature. Journal of Building Materials,1-12.
3. He, B., Zhang, H. E., Zhao, M. R., et al. Tensile behavior and acoustic emission damage temporal evolution of UHPC under ultra-low temperature-high temperature alternating environment. Journal of Building Structures,2024,45(09):1-12.DOI:10.14006/j.jzjgxb.2023.0529.
4. Zhang, T. Application of jacked pipe construction technology under urban traffic main roads. Stone Industry,2024,(08):132-134.DOI:10.14030/j.cnki.scaa.2024.0385.
5. Li, J. F. Research on early shrinkage deformation and crack development law of ultra-high performance concrete. Northeast Electric Power University.,2023.DOI:10.27008/d.cnki.gdbdc.2023.000201.
6. Jian, M. (2023). Research on composition design and bonding performance of basalt fiber reinforced ultra-high performance concrete. Yangzhou University.,2023.DOI:10.27441/d.cnki.gyzdu.2023.002476.
7. Yan, X. Y., Yu, C., & Zhai, S. H. Experimental study on mechanical properties of joints of segmented prefabricated pipe gallery segments. Sichuan Building Science Research,2017,43(06):28-31.
8. Liu, L. B. Performance and structural analysis of ultra-high performance concrete composite pipe. Wuhan University of Technology,2018.
9. Yang, Y., Chen, R., Huang, Q. W., Chen, B. C., Huang, W., & Wei, J. G. Optimization design and life-cycle cost analysis of UHPC pipe gallery. Journal of Ningxia University (Natural Science Edition),2018,39(03):227-233.

10. Lu, L. Research on reinforcement method of shield tunnel segments with ultra-high performance concrete (UHPC). Hunan University,2019.
11. Chen, R. P., Lu, L., Zhang, Y., & Wu, H. N. UHPC reinforcement technology and mechanical performance analysis of shield segments. Engineering Mechanics,2019,36(11):41-49.
12. Liu, X., Zhang, J. L., Jiang, Z. J., Liu, Z., Xu, P., & Li, F. Experiment on UHPC reinforcement of shield tunnel lining structure. China Journal of Highway and Transport,2021,34(08):181-190.
13. Zhang, Y., Huang, S. L., Liu, Y. F., & Shao, X. D. Experimental study on flexural performance of RC beams reinforced with prestressed UHPC. Journal of Hunan University (Natural Sciences),2022,49(03):23-31.
14. Zhou M ,Zhao X ,Song J , et al.Seismic performance of precast UHPC pipe pile with two pile-cap beam connection types: An experimental and numerical study.Soil Dynamics and Earthquake Engineering,2024,186108900-108900.
15. JinJing L ,Xin-Chao L ,De-Hua Z , et al.Behavior of FRP grid-reinforced ultra-high performance concrete (UHPC) pipe under lateral compression.Case Studies in Construction Materials,2023,19
16. Jabbar M A ,Zuheriy A S A ,Hasan A Q .A numerical investigation of the structural behavior of reinforced concrete beams fully or partially encased with UHPC layers in flexure.Structures,2024,70107706-107706.
17. Song B, Liu F. Finite element analysis of flexural performance of reinforced ultra-high performance concrete beams. Concrete and Cement Products,2022,(06):58-61.DOI:10.19761/J.1000-4637.2022.06.058.04.